New electrooptic polymer configuration for high frequency modulators and digital signal processing applications

Harold R. Fetterman*[a], Byoung-Joon Seo, Bartosz J. Bortnik, Yu-Chueh Hung , Seongku Kim
[a]University of California at Los Angeles, Electrical Eng. Dept., Los Angeles, CA, USA 90024

Abstract

Recent advances in polymer materials have significantly increase the available electrooptic coefficients. This has now stimulated the development of new designs and configurations for high frequency optical modulators. In addition, it has opened up the field to new applications including high speed optical Digital Signal Processing. The initial areas investigated include linear modulators, true time delays and arbitrary waveform generation. More complex devices with multiple elements in series are now being investigated.

Keywords: Polymer modulators, Linearized modulators, Ring resonator modulators, Optical Digital signal processing,

1. INTRODUCTION

The use of electrooptic polymers for making modulators and related devices has been growing now that the magnitude of the effect has significantly increased over Lithium Niobate. These materials have been incorporated into devices with low operating voltages and high frequency capabilities. Some of the most recent devices we have examined include modulators using coupled optical guides for high linearity and ring resonators for ultra high speed operation. An extension of this approach is to make a basic unit capable of performing optical digital signal processing. In this application many of the concepts used in electrical DSP can be optically implemented. However, because of the speed inherent in the optical response these devices are capable of extraordinary frequencies. The natural capability of optical systems for parallel configurations also adds to the future potential of these systems.

I.2 Device Development

We have recently developed novel photonic devices using electro-optic polymer waveguides. They are ring resonator-based modulators, linearized modulators and optical digital switches. We have also investigated passive-to-active transitions to minimize the propagation loss in making complex devices with several stages. The traveling-wave ring resonator-based modulator is a new design of optical modulators for high speed operation. It is intrinsically fast due to the reduced drive interaction length obtained using optical resonance. We have demonstrated modulation speeds up to 165 GHz[1]. The schematic diagram and modulation characteristics for this device are shown in Figure 1.1. Since related ring structures used in this device are also a part of our OSPs, we believe that operation speed of the OSPs will be comparable.
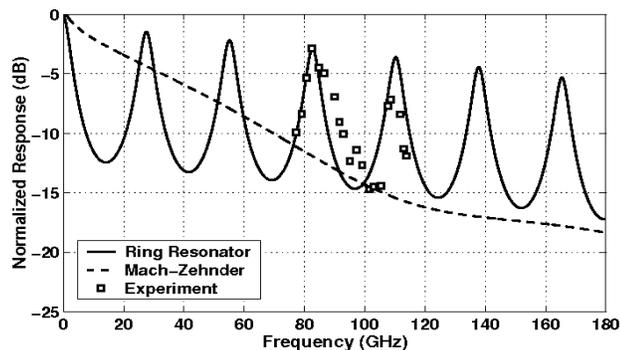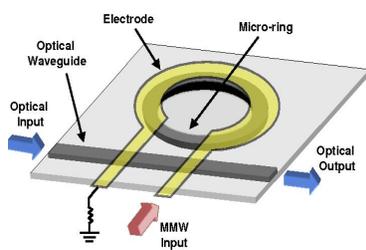
Figure 1.1 Schematic diagram of the traveling-wave ring resonator-based modulator and its modulation characteristics. We have demonstrated its modulation speed up to 165 GHz.

Another device we have developed using electro-optic polymers are the linearized modulators[2] shown in Figure 1.2. They are based on directional coupler modulators with two different coupling sections. The two different coupling sections make the modulation response linear by effectively canceling the nonlinear portion of the modulation process. We have fabricated the different coupling sections by using a novel photo-bleaching method[3]. The photo-bleaching method is our previously developed way of defining waveguides and it is simple and greatly reduces the optical losses due to RIE fabrication.
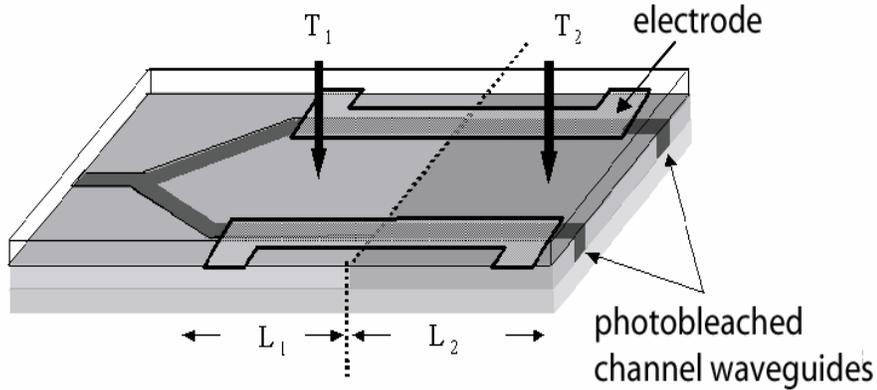
Figure 1.2 Schematic diagram of the direction coupler linearized modulator. Two different coupling sections are defined with the photo-bleaching technique, which reduces the nonlinear terms in the response function.

We have also developed 1x2 and 1x4 digital optical switches (DOS)[4]. An example of these is the single input, four output device shown in Figure 1.3. It switches the input light to one of the four outputs using a configuration of three individual 1x2 DOSs. The schematic and switching characteristic of one of the 1x2 DOS building blocks device is shown in Figure 1.4. We employed passive-to-active hybrid waveguides to reduce the total propagation loss in this implementation. We used DH6/APC (Lumera Co.) for the active electro-optic polymer material and SU-8 (MicroChem Co.) for the low loss passive material at 1.3 microns.
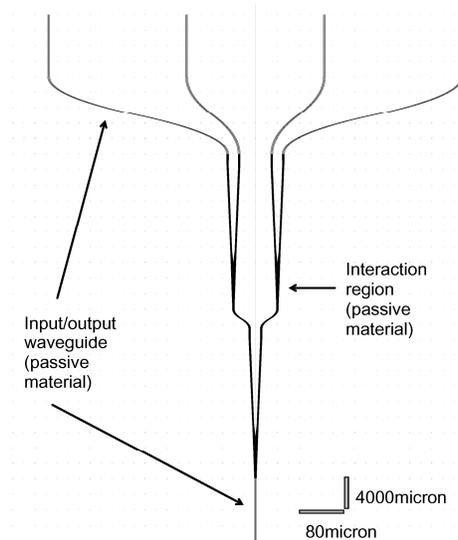
Figure 1.3 Hybrid passive-to-active 1x4 digital optical switch (DOS). It switches the input light to one of four outputs configured using three individual DOSs.
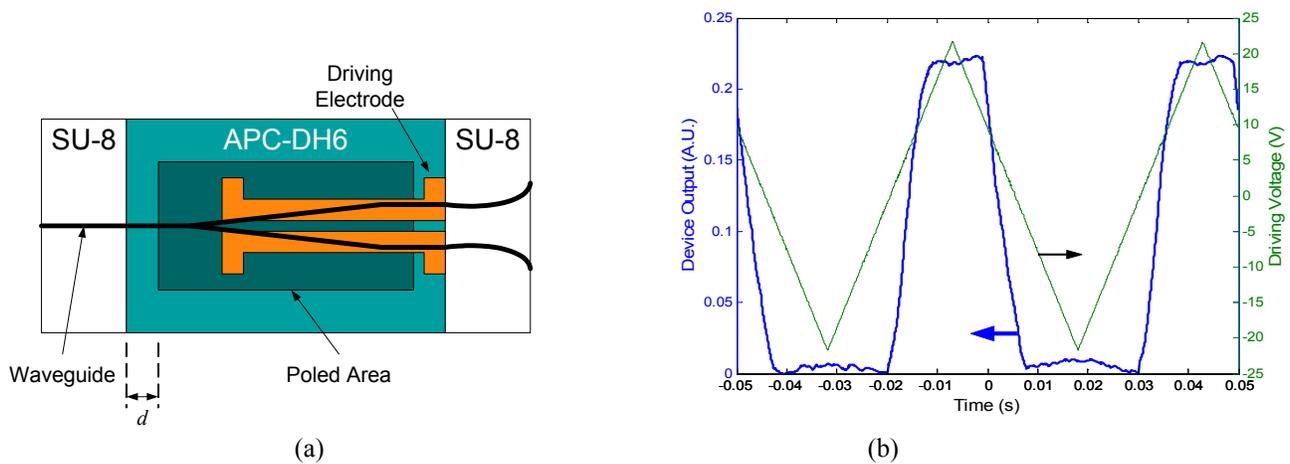
Figure 1.4 (a) Schematic diagram for 1x2 DOS. It employes hybrid passive-to-active transitions to reduce the propagation loss. (b) Switching characteristics for the 1x2 DOS. The switch turns on and off with 14V using single sided activation.

One of the most important recent developments in our laboratory is the serial passive/active transition waveguide for polymer structures. In order to generate the more arbitrary and complex functions, a large number of unit structures in series are required. The optical loss limits the possible number of unit blocks in this configuration. In an effort to overcome the propagating loss limitations of electro-optic polymers, various types of passive-to-active transition techniques have been studied in our group[5]. Our most recent approach is to use passive low loss polymer materials, with an integrated butt coupling, in the same plane as the active electrooptic materials. As shown in Figure 1.5 the higher loss active materials are only used in areas where active control is needed.. The refractive index of the low loss passive material (LP73, Lumera Co.) is 1.55 and the material propagation loss is about 0.5 dB/cm at 1.55 μm. Since its refractive index from the core material (DH6/APC1, Lumera Co., index = 1.612 at 1.55μm for the TM mode) is very similar, we find the coupling loss can be negligible with a relatively simple style butt coupling. Figure 1.5 shows a microscopic image of our passive/active transition devices. The transition loss for this device is measured to be approximately 1 dB. The 1 dB loss is due to scattering at the passive/active junctions, which can be minimized in our future fabrication approaches.
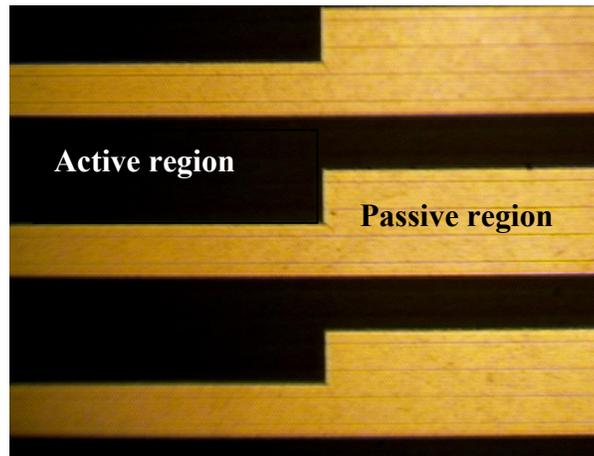
Figure 1.5 Microscopic image of the Active/Passive Transition device. The optical signal transits between a low loss passive polymer waveguide and the active polymer material with the butt coupling. We are currently pursuing minimizing scattering loss at the junctions.

II. Review of Optical Signal Processor

We are currently developing new OSPs, such as discussed by Madsen [6], using hybrid electro-optic polymer waveguides. In this section, we review their fundamental concepts and discuss the capability of our latest OSP devices.

II.1 Theory Review of OSP

The fundamental working idea of OSPs lies in the multiple temporal interference of delayed optical signals. By controlling the amplitude and the phase of the interfering signals, the optical signal can be processed in an arbitrary way. Several physical values are important for characterizing an OSP. They are the unit time delay and the number of arms that split or combine light. The unit delay time, $\Delta\tau$, represents a time resolution for an OSP to process a signal. Due to this time resolution, the frequency response of an OSP is periodic and the period is proportional to $1/\Delta\tau$. This period is called the free spectral range (FSR). The number of light splitting and combining arms determines the spectral resolution of the OSP within the FSR. As the number of arms increases, higher resolution frequency responses can be obtained and hence more arbitrary responses are possible. An arm can be classified into two types; forward feeding arms and backward feeding arms. Since the response of forward feeding arms are finite in time, they are called finite impulse response (FIR). In the similar way, the response of backward feeding arms are called infinite impulse response (IIR) since they are infinite in time. The number of forward feeding arms and of backward feeding arms represent the order of the FIR and the IIR of the OSP.

In the usual treatments x(t) and y(t) are used to denote the input and output signal respectively. An OSP performs an operator to transform the input x(t) into the output y(t). Several methods can be used for describing an OSP. The first method is to use a characteristic equation. If an OSP has M forward feeding arms and N backward feeding arms, the characteristic equation of the processor can be generally written as,

$$y(t) - \sum_{k=1}^{N} b_k \, y(t - k\Delta\tau) = \sum_{k=0}^{M} a_k \, x(t - k\Delta\tau) \qquad (2.1)$$

The coefficients, a_m and b_n, stand for the amplitude and phase changes of the m'th forward feeding arm and the n'th backward feeding arm respectively. The coefficients are complex values in general because the signals, x(t) and y(t), stand for coherent optical fields and thus have both amplitude and phase.

II.2 OSP using Electro-optic Polymer waveguides

The unit block, we have chosen in our current work consists of a symmetric Mach-Zehnder interferometer and a race-track waveguide as shown in Figure 2.1. "Symmetric" means the lengths of the two waveguide arms of the Mach-Zehnder interferometer are same. Actually a race-track structure is used so that the straight waveguide section has an extended coupling region for coupling inside and outside of the ring.
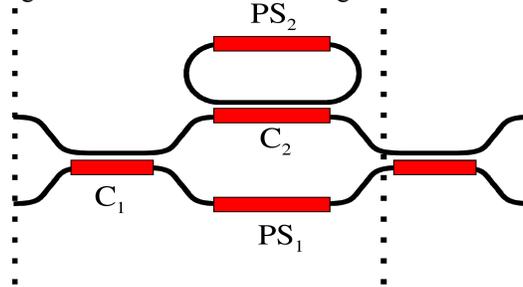
Figure 2.1 Unit Blocks of the OSP proposed. It is a two-port input and two-port output system. It consists of a symmetric Mach-Zehnder interferometer and a mouse track waveguide. Four electrodes control the locations of a zero and a pole.
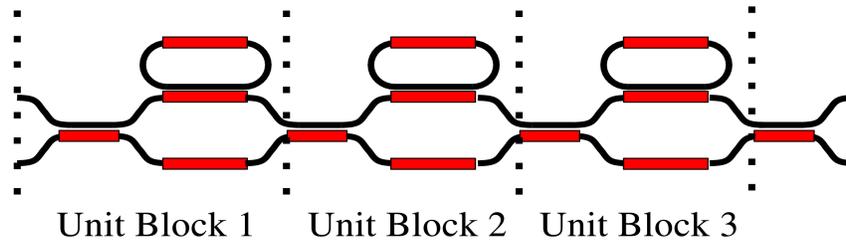
Figure 2.2 Multiple structure of OSP. It consists of N cascaded unit blocks

This unit block, originally proposed by K. Jinguji[7], has two input ports and two output ports. Any input port can be used for operation while the two output ports are related each other in a conjugate power relation. A conjugate power relation means that the total sum of two output powers is the same as the input power if the system is lossless.

Our unit block therefore contains two configurable couplers and two phase shifters. They are labeled as C1, C2, PS1 and PS2 as shown in Figure 2.1. In order to have a useful phase shift at PS2, the perimeter of the race-track must be large enough. We designed the radius of the race-track to be 1 mm. The interaction lengths of C2 and C1 range from 100 μm to 4 mm and 6 mm, respectively. Separations of waveguides for the C1 and C2 couplers are 5 μm and 2 μm.
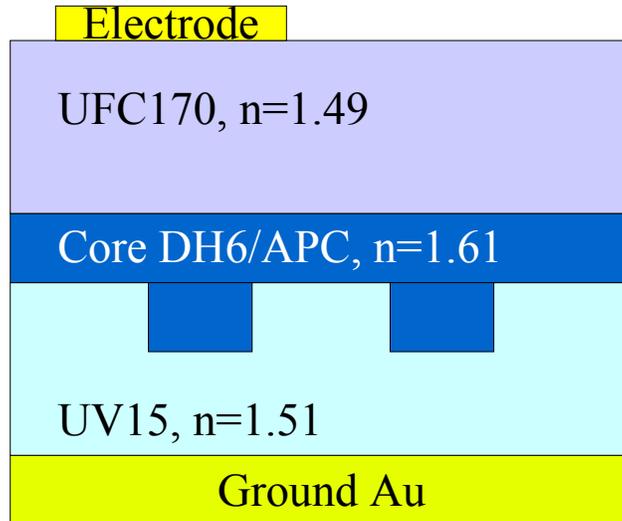
Figure 2.3 Cross section view of OSP at couplers. UFC170, DH6/APC and UV15 are used for upper cladding, active core and lower cladding layers respectively. The Inverted waveguide is designed to reduce scattering due to wall roughness at the waveguide rib.

For the electro-optic polymer core material, DH6/APC (Lumera Co.) is used. The single layer films of DH6/APC have shown a high electro-optic coefficient r_{33} of 70 pm/V at 1.31 μm. For the lower and upper cladding polymers, UV15LV (Master Bond Co.) and UFC170A (Uray Co.) are used. The indices at 1.55 μm of the core, lower and upper claddings have been measured to be 1.61, 1.51 and 1.49, respectively. Using these indices, the waveguide structure with 2 μm width, 1 μm high rib and 1 μm high slab has been designed. The inverted rib structure was chosen since this waveguide structure[8] minimizes the scattering loss from the sidewall roughness and Figure 2.3 shows the cross section of the waveguides at the coupler section.

Even though the OSP is compact in size, several components are integrated. In order to operate an OSP properly, all components inside the OSP must operate properly. For verification purposes of these components, we individually tested
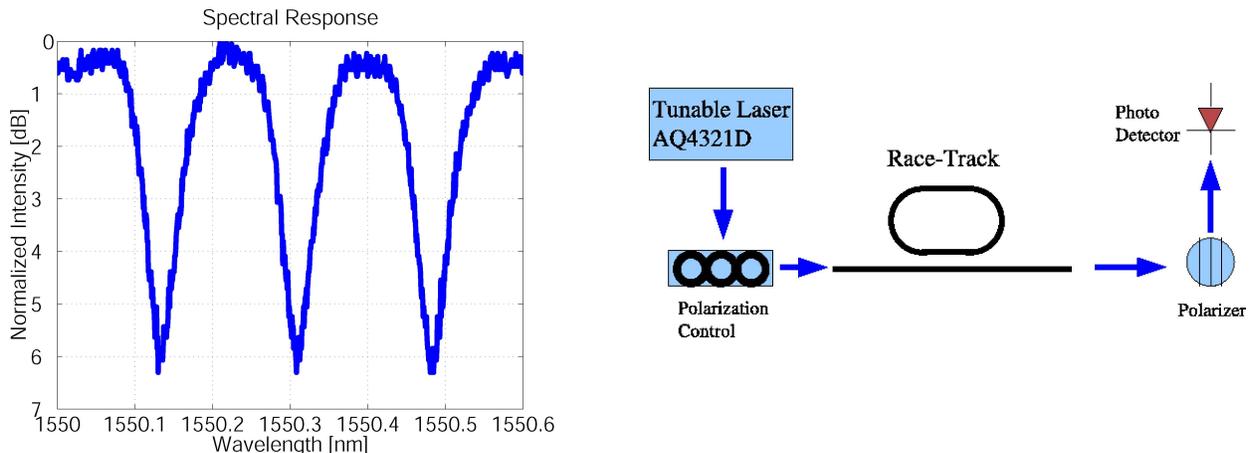
Figure 2.4 (a) Spectral response of a race-track. The free spectral range, extinction ratio, fitness and Q-factor are measured 0.22 nm, 6 dB, 3.7 and 2.6×10^4, respectively. (b) Experimental setup for the race-track spectral response measurement for (a).

their performances. The individual tests include the race-track measurements, C1 (and C3) coupler measurement and measurements for the two phase shifters (PS1 and PS2), which are discussed below.

Figure 2.4 shows the spectral response of a race-track structure and its experimental measurement setup. The racetrack measured has a bending radius and coupler length of 1 mm and 100 μm, respectively. A Q4321D (Ando) is used for the tunable laser source at 1.55 μm with TM mode polarization control. As seen in Figure 2.4(a), the measurement is done in a 0.6 nm wavelength span and the free spectral range (FSR), extinction ratio, finesse and Q-factor are measured to be 0.22 nm, 6 dB, 3.7 and 2.6×10^4, respectively. Using these values, the optical effective refractive index, total round trip optical loss and the optical loss inside the ring are calculated as 1.66, 2.16 dB and 3.33 dB/cm respectively. The transmission coefficient of the coupler has also calculated with these values to be 0.48. This value is somewhat smaller than the expected value due to the fabrication tolerances.

The racetrack measured has a bending radius and coupler length of 1 mm and 100 μm, respectively. A Q4321D (Ando) is used for the tunable laser source at 1.55 μm with TM mode polarization control. As seen in Figure 2.4(a), the measurement is done in a 0.6 nm wavelength span and the free spectral range (FSR), extinction ratio, finesse and Q-factor are measured to be 0.22 nm, 6 dB, 3.7 and 2.6×10^4, respectively. Using these values, the optical effective refractive index, total round trip optical loss and the optical loss inside the ring are calculated as 1.66, 2.16 dB and 3.33 dB/cm respectively. The transmission coefficient of the coupler has also calculated with these values to be 0.48. This value is somewhat smaller than the expected value due to the fabrication tolerances.

We then characterized the components inside the OSP. Figure 2.5 shows the experimental setup. The components were modulated by applying a 40 V peak-to-peak triangular volt signal into the individual electrodes. Figure 2.6 shows the modulation characteristics for C1, PS1 and PS2, respectively.
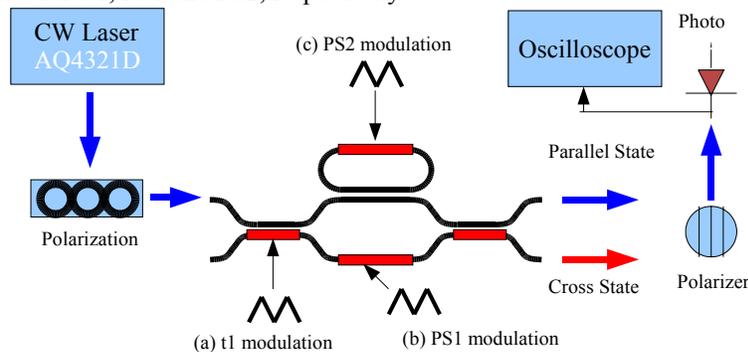
Figure 2.5 Experimental setup for individual components' characterization. The 40 peak-to-peak triangular signal is applied to C1, PS1 and PS2 and optical responses are measured.
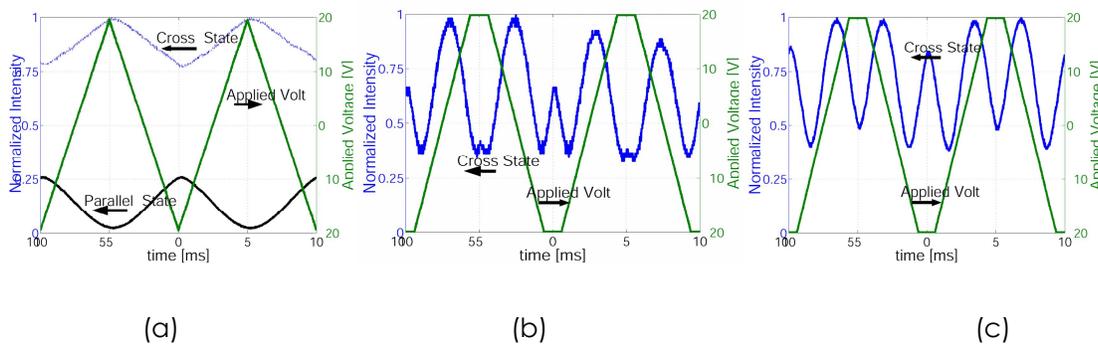
Figure 2.6 (a) Parallel and cross state transmission when a 40 peak-to-peak triangular signal is applied to C1. The transmission coefficient for C1 coupler is estimated as 0.6 and it has a tuning range of ±0.15 when applied voltage is ±20 V. (b and c) Cross state transmission when the signal is applied to PS1 and PS2, respectively. They show that the half-wave voltages of PS1 and PS2 are 33 V and 30 V, respectively.

As indicated in Figure 2.6(a), the transmission coefficient for C1 is estimated as 0.6 and it has tuning range of ±0.15 when the applied voltage is ±20 V. Figure 2.6(b) and Figure 2.6(c) show that the half-wave voltages of the PS1 and PS2 phase shifters are 33 V and 30 V, respectively. Since the electrodes separation is about 10 μm and the interaction lengths for two phase shifters are 5 mm and 6 mm, respectively, these half-wave voltage corresponds to r33 coefficient of around 30 pm/V.

III. High Speed Analog Applications

III.1 Arbitrary Waveform Generator

Researchers have shown[9] that using PLC structures which are similar to OSP structures, it is possible to implement arbitrary optical filters. These filters can be designed for arbitrary transfer functions in phase as well as amplitude. For example, we can generate linear dispersion for a notch filter. Such filters have been experimentally investigated in silicon, where thermal tuning was used to change the index of refraction. Since our OSP are based on the electro-optic effect, much higher data rates (more like tens of gigahertz) will be accessible. This device will have applications to modulator linearization and correction for amplifier distortion.

Using a sinusoidal input, the OSP generates the desired output shape with proper adjustment of the parameters; C1, C2, and PS1. However, the desired output shapes should be symmetric at its maximum when a sinusoidal input is used. Figure 3.2(b) shows a computer simulation of an OSP generating a rectangular waveform signal. The OSP considered has a single block as shown in Figure 3.2(a) and round trip loss inside the ring waveguide of 3 dB is assumed. Taking the individual parameters labeled in the figure, a sinusoidal voltage input, whose maximum voltage corresponds to Vπ/2, is assume to be applied to the electrode on top of the ring waveguides. As shown in the figure, the overall intensity follows the rectangular shape. As the number of unit blocks increases, the more rectangular the shape will be. Furthermore, this waveform can be quickly changed to another desired shape with different sets of parameters due to the speed of the electro-optic effect.

(a)   (b)
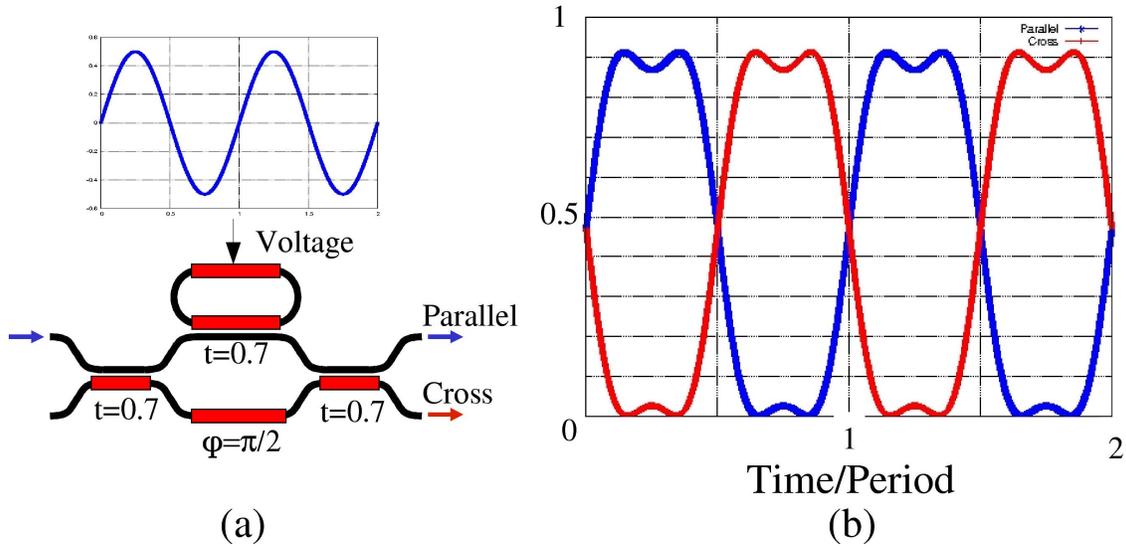
Figure 3.2 (a) Single block OSP is configured to generate a rectangular waveform signal. A sinusoidal voltage signal, whose maximum voltage is half of Vπ, is assumed applied to the electrode on top of the ring waveguide and the individual parameters used are labeled accordingly. (b) Generated rectangular waveform signal using one unit block. As the number of unit blocks increases, the more rectangular the shape will be.

III.2 Linearized Modulator

Another useful application of the OSP is a linearized electro-optic modulator. Electro-optic modulators are one of the most important devices of lightwave communication. The most common scheme for this device is to use the Mach-Zehnder interferometer. However, the inherent disadvantage of this technique is a large nonlinear distortion limiting the dynamic range in analog applications. Several approaches have been attempted for increasing the dynamic range of the modulator. They are usually based upon optical waveguide couplers utilizing the nonlinear response of the coupling coefficient to the applied electric field.

The OSP can also perform as a linearized amplitude modulator if the applied electric field modulates the optical phase inside the ring. The fundamental concept for the linearized modulator in this structure lies in the nonlinear response of the optical phase to the applied electric field. The optical phase change inside the ring recursively changes the overall optical phase leading to a nonlinear response. This feature is related to the arbitrary waveform generator as discussed in Section III.1. The linear amplitude response is just another kind of arbitrary waveform generation.

(a)   (b)
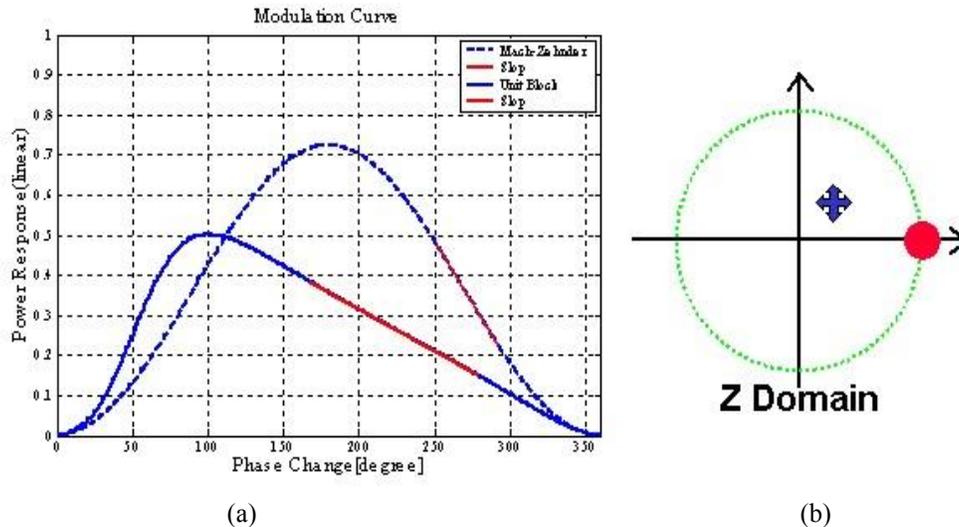
Figure 3.4 (a) Linearized Transfer function of OSP. It is compared with the conventional MZ modulator. (b) Optimized Zeros and Poles Location. The linear modulation occurs outside the resonance region.

VI. Conclusion

During the current work we have demonstrated the concept of using a unit block approach for OSP. We have also shown that the basic concept can be made using the current state of polymer technology. We have now made several prototype ODSP devices which indicate important potential applications. They will now be engineered to operate at high speed where no competitive technology exists. We believe that by going to DOSP the systems will be much more robust than any electronic implementation. The systems will be smaller, much lower in power consumption, and have capability far exceeding current electronic approaches. This effort represents a major step in a new generation of optical applications.

[1] B. Bortnik, Y.-C. Hung, H. Tazawa, B.-J. Seo, J. Luo, A. K.-Y. Jen, W. H. Steier, H. R. Fetterman, "Electrooptic Polymer Ring Resonator Modulation up to 165 GHz", J. of Selected Topics in Quantum Elect., v13, #1, pp.104-110, 2007.

[2] Yu-Chueh Hung. Fetterman HR., "Polymer-based directional coupler modulator with high linearity", IEEE Photonics Technology Letters, Vol.17, No.12, pp.2365-2567, Dec. 2005.

[3] Kim Seongku, Geary K., Fetterman H.R., Zhang C., Wang C., and Steier W.H. , "Photo-bleaching induced electro-optic polymer modulators with dual driving electrodes operating at 1.55 m wavelength", Electronics Letters, Vol. 39, Issue 18, pp.1321-1322, 4 Sep. 2003.

[4] Wei Yuan, Seongku Kim, Fetterman HR., "Low-loss interconnection between electro-optic and passive polymer waveguides for planar lightwave circuits", Microwave and Optical Technology Letters, vol.48, no.3, pp. 415-18. 2006

[5] Wei Yuan, Seongku Kim, H. R. Fetterman, W. H. Steier, D. Jin, R. Dinu, "Hybrid Integrated Cascaded 2-bit Electrooptic Digital Optical Switches (DOS)," Photonics Technology Letters, v19, #7, pp519-521, 2007

[6] C. K. Madsen and G. Lenz, "Optical all-pass filters for phase response design with applications for dispersion compensation," IEEE Photonics Technology Letters, v10, pp.994-996, Jul 1998

[7] K. Jinguji, and M. Kawachi "Synthesis of coherent two-port lattice-form optical delay-line circuit" IEEE Journal of Lightwave Technology, v13, pp73-81, Jan 1995

[8] Seong-Ku Kim, H. Zhang, D. H. Chang, C. Zhang, C. Wang, W. H. Steier, and H. R. Fetterman,"Electrooptic Polymer Modulators With an Inverted-Rib Waveguide Structure", IEEE Photonics Tech. Letters, Vol. 15, No. 2, pp.218-220, Feb. 2003

[9] M. R. Fetterman and H. R. Fetterman, "Optical Device Design With Arbitrary Output Intensity as a Function of Input Voltage", IEEE Photonics Tech. Letters, Vol. 17, No. 1, pp 97-99, Jan. 2005